How Nitrogen seeding securizes plasma ramp-up in the metallic environment of WEST

P. Maget, J-F Artaud, C. Bourdelle, J. Bucalossi, H. Bufferand, G. Ciraolo, C. Desgranges, P. Devynck, D. Douai, R. Dumont, N. Fedorczak, F. Felici[1], M. Goniche, C. Guillemaut, R. Guirlet, J. Gunn, I. Ivanova-Stanik[2], T. Loarer, P. Manas, J. Morales, P. Moreau, R. Nouailletas, C. Reux, O. Sauter[1], S. Van Mulders[1] and the WEST team*

CEA, IRFM, F-13108 Saint Paul-lez-Durance, France. [1] *EPFL, Swiss Plasma Center (SPC), CH-1015 Lausanne, Switzerland,* [2] *Institute of Plasma Physics and Laser Microfusion, 01-497 Warsaw, Poland.* * *see http://west.cea.fr/WESTteam*

Summary The plasma ramp-up phase can be critical in metallic wall tokamaks, due to the potentially large core radiation and limited additional heating available in this phase. Nitrogen seeding has been used on WEST to help peaking the electron temperature and plasma current, and avoid the formation of a low core temperature with current profile distribution prone to MHD mode triggering. In the context of a contamination by Tungsten, that has a maximum cooling rate at about 1.5 keV, moving above this peak is particularly important. Integrated simulations with the RAPTOR code coupled to the Qualikiz Neural Network help understanding experimental observations: increasing the light impurity content in the edge region triggers an improved confinement via dilution effect and equilibrium modification that leads to both higher core temperature, higher core current and better MHD stability.

Experimental observations We show in figure 1 an example of a series of L-mode discharges with different Nitrogen injection rates between plasma breakdown and the flat top at $I_p = 0.5MA$. While in the absence of Nitrogen seeding the core plasma temperature remains low at about 1 keV, with several signs of MHD activity, it rises to about 2 keV when the Nitrogen injection rate is at 0.1 Pa.m$^3/s$. The temperature profiles at $t = 2s$, shown in figure 2, demonstrate that the effect of the light impurity seeding is particularly important in the central part of the plasma, while the edge region shows little modification.

Global plasma parameters collected on a selected database with similar plasma conditions show a nice correlation of the core temperature and internal inductance increase with the quantity of Nitrogen injected up to $t = 2s$ or $t = 3s$ (expressed in Pa.m^3), as shown in figure 3. The core temperature is typically in the range of maximum cooling rate for Tungsten. In spite of the inevitable increase of the effective charge Z_{eff} of the plasma due to the assimilation of Nitrogen ions to the plasma evidenced by visible and UV spectroscopy, the ohmic power is rather constant, while the total radiated power shows a moderate increase. The behavior of the ohmic power demonstrate that the gain in plasma conductivity due to the higher temperature compensates for increased effective charge of the plasma.

The analysis of Langmuir probe measurements when Nitrogen is injected shows temperatures falling down to few eV on the divertor, indicating a detached regime that ends before $t = 3s$ as the plasma

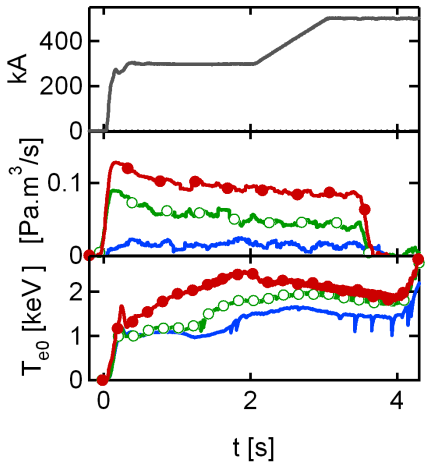

Figure 1: *Pulses with increasing Nitrogen seeding rate: plasma current, Nitrogen injection rate and electron temperature.*

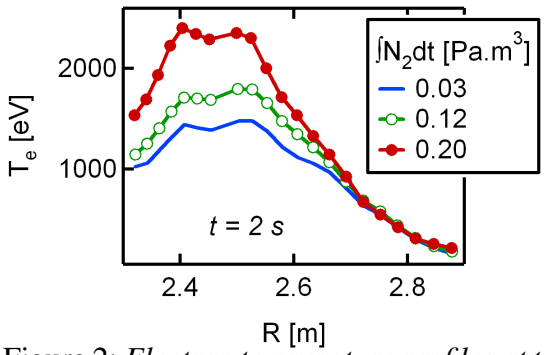

Figure 2: *Electron temperature profiles at $t = 2$s for the three discharges of figure 1.*

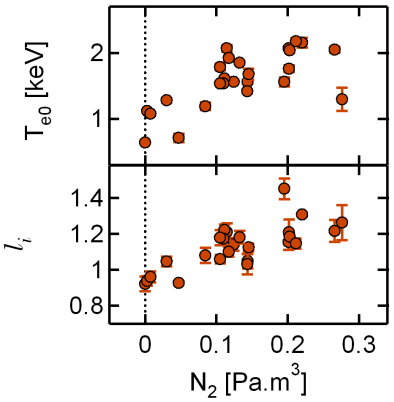

Figure 3: *Core temperature and internal inductance vs injected Nitrogen at $t = 2s$ (exp.).*

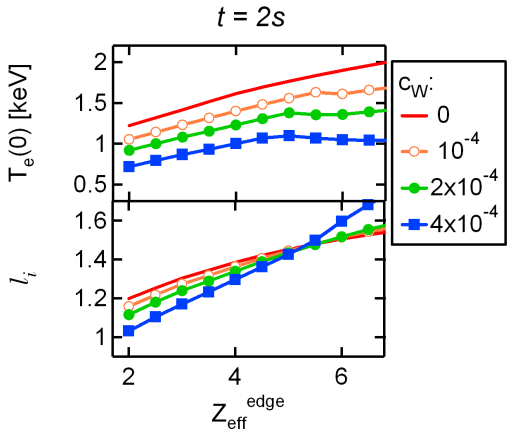

Figure 4: *Core temperature and internal inductance vs Z_{eff}^{edge} at $t = 2s$ (RAPTOR).*

current increases. This detached condition is confirmed by visible spectroscopy with Tungsten sputtering (evaluated from WI/DI signals) remaining extremely low in this phase, while at $t = 3s$ the presence of increasing levels of Nitrogen is correlated with an increasing Tungsten sputtering (fig.5). Besides these observations at the divertor, the contamination of the plasma remains however independent on the Nitrogen injection (fig. 6), highlighting the instrumental contribution of screening effects [1]. The inferred Tungsten relative concentration in the core is in the range $c_W \in [0.5 \times 10^{-4}, 2 \times 10^{-4}]$.

Integrated modelling Early Nitrogen injection experiments are modelled with the RAPTOR code [2, 3] coupled with the 10D Neural Network QLK-NN [4] for turbulent heat transport, with Deuterium and Nitrogen ions taken into account for the electroneutrality, while Nitrogen as well as Tungsten are taken into account for the radiative losses. The observed decay of ohmic power as Nitrogen is injected requires considering a hollow profile of Z_{eff}, which we take as parabolic, with a core value $Z_{eff} = 2$

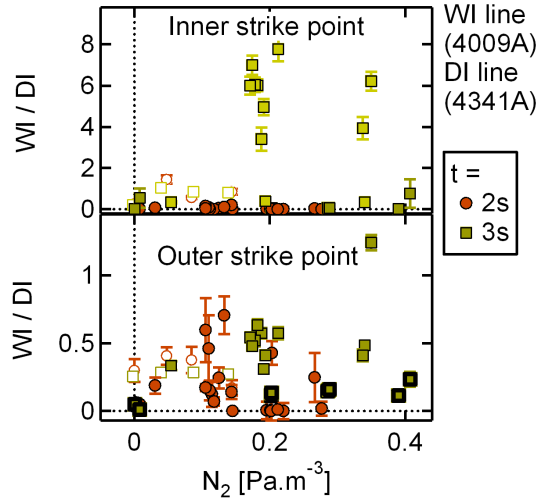

Figure 5: *Normalized Tungsten WI emission.*

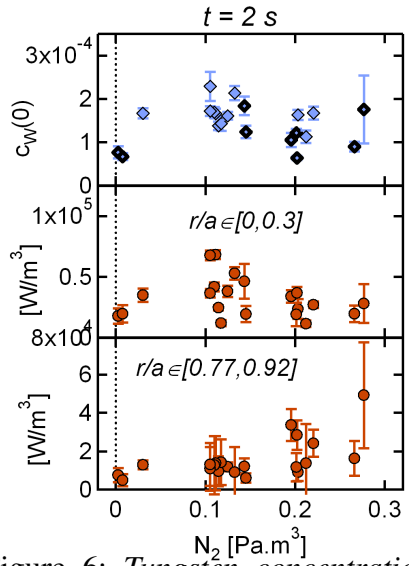

Figure 6: *Tungsten concentration, core and edge radiative power density.*

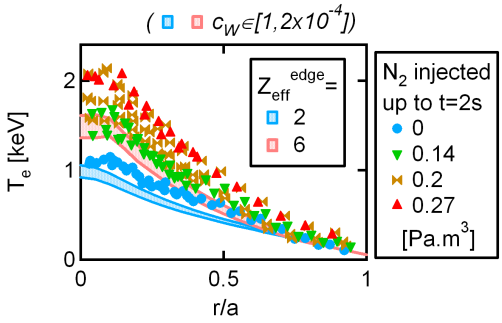

Figure 7: *Experimental and simulated T_e profiles.*

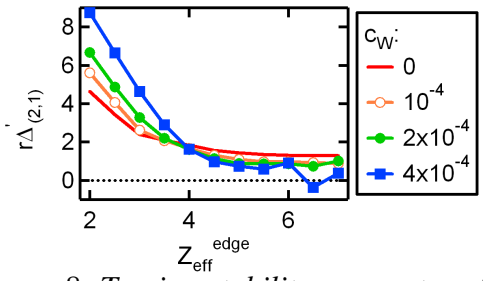

Figure 8: *Tearing stability parameter $r\Delta'$ for (2,1) island.*

that corresponds to the resistive evaluation in a typical non-seeded experiment. Nitrogen injection is then modelled by increasing the edge value of Z_{eff}. The radial boundary condition is set at $r/a = 0.8$ since QLK-NN underestimate turbulent outside this position, possibly because resistive modes (not included in the model) play a role there (discharges are in L-mode). The Porcelli sawtooth model [5] with full reconnection is used to limit the current density in the plasma core. In the following, we focus on the effect of Nitrogen seeding at $t = 2s$, taking as reference a pulse without Nitrogen seeding.

The comparison of electron temperature profile from the experiment and the simulation with a flat Z_{eff} (no seeding) shows a relatively good agreement, although the effect is underestimated by about 25% in the simulations (fig. 7). The increase of the core electron temperature is accompanied by a concomitant change in the internal inductance (fig. 4). The change in the (2,1) tearing mode stability parameter $r\Delta'$, shown in fig. 8, goes in the direction of an improved MHD stability with respect to magnetic island triggering, in agreement also with experimental observation. The physics mechanism leading to this result can be evidenced by considering (i) the change in the normalized temperature gradient, and (ii)

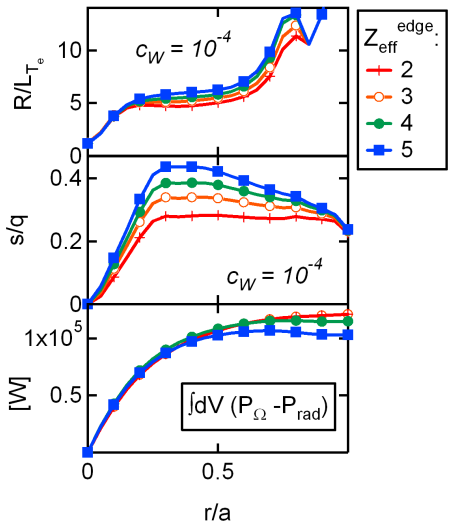

Figure 9: *Normalized temperature gradient, s/q and cumulative net power profiles at $t = 2s$ for $c_W = 10^{-4}$.*

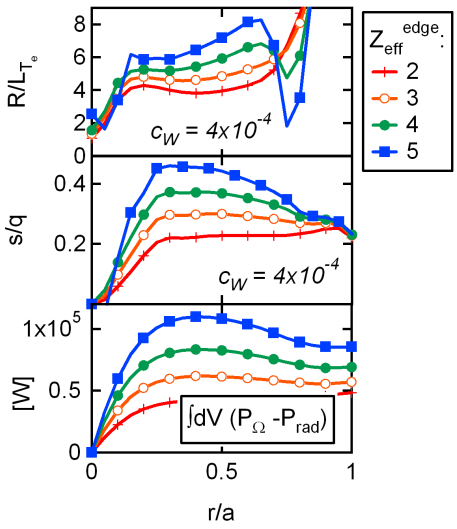

Figure 10: *Normalized temperature gradient, s/q and cumulative net power profiles at $t = 2s$ for $c_W = 4 \times 10^{-4}$.*

the change in the net power balance. As shown in figures 9 and 10, the main reason for the favorable of Nitrogen seeding comes from the increase of turbulence threshold (R/L_{Te}) on most of the plasma radius. Part of this improvement can be attributed to the induced change in the magnetic equilibrium, as shown by the increase of s/q consistent with an up-shift of TEM/ITG threshold [7]. The dilution effect certainly contributes as well (determining its relative amplitude requires dedicated computations), as already documented on WEST [6]. At low Tungsten contamination, both R/L_{Te} and the power balance are unchanged in the plasma core. When the plasma is contaminated by Tungsten, the core power balance is however greatly improved as more Nitrogen is injected, due to the large increase of the ohmic power source induced by a larger core current density.

Conclusion The beneficial effect of Nitrogen seeding during the plasma ramp up in WEST is explained using integrated RAPTOR simulations with QLK-NN by the reduction of turbulent transport induced by a combination of the direct effect of dilution and the indirect effect of the peaking of the current density. When Tungsten contamination is large, an increase of the net heat source in the plasma core is also evidenced. The change in the magnetic equilibrium also results in a better stability of magnetic islands, consistent with experimental observations.

References

[1] Y. Marandet et al., Contributions to Plasma Physics, 54 (2014) 353.
[2] F. Felici et al., Nuclear Fusion 51 (2011) 083052.
[3] F. Felici et al, Nuclear Fusion 58 (2018) 096006.
[4] K.L. van de Plassche et al., Physics of Plasmas 27 (2020) 022310,
[5] F. Porcelli et al., Plasma Physics and Controlled Fusion 38 (1996) 2163.
[6] X. Yang et al., Nuclear Fusion 60 (2020) 086012.
[7] C. Fourment et al., Plasma Physics and Controlled Fusion 45 (2003) 233.